

Blinking photoluminescence properties of single TiO₂ nanodiscs: interfacial electron transfer dynamics†

Ki-Seok Jeon,^{ab} Seung-Do Oh,^a Yung Doug Suh,^b Hiroyuki Yoshikawa,^c Hiroshi Masuhara^{cd} and Minjoong Yoon^{*a}

Received 18th July 2008, Accepted 16th September 2008

First published as an Advance Article on the web 6th November 2008

DOI: 10.1039/b812361f

Blinking photoluminescence was observed in single TiO₂ nanodiscs (NDs) by using a laser scanning confocal microscope (LSCM)-coupled steady-state and ps-time-resolved photoluminescence (PL) spectroscopic system, while it was not significantly observed for TiO₂ quantum dots (QDs). Analysis of the PL blinking time trajectories revealed single-exponential kinetics with the average lifetimes of on-state (~286 ms) and off-state (~58 ms), implying the existence of inherent surface-trap sites which can be filled by photogenerated electron or hole. The PL spectra of single TiO₂ NDs exhibited broad surface emissions with four decay times, which may be due to diffusion of the energies of electron or hole trap states related to surface structural changes by modification of TiO₂ QDs. These results and the surface structural analysis (IR and XPS) suggests a simple model for the PL blinking of single TiO₂ NDs that is based on repetitive interfacial electron transfer to the inherent surface trap sites ($4\text{Ti}^{4+}\text{-OH}$) with Auger-assisted hole trapping in the multiple surface states as modified by the diffusive coordinate model and the surface-trap-filling model. Based on this blinking mechanism and kinetics, the rates of the interfacial electron transfer and the back electron transfer in TiO₂ NDs were determined to be 18 ns and 58 ms, respectively, which are slow enough to keep the polarization of e–h pairs at the surface for efficient photocatalysis and photovoltaic activities. The present methodology and results may be applicable to obtain surface exciton dynamics of various photoelectronic semiconductor nanostructures.

1. Introduction

TiO₂ nanoparticles have been attracting a great deal of attention due to their potential applications for the development of photocatalysts and photovoltaic devices useful for solar energy conversion, water splitting for hydrogen generation, degradation of environmental pollutants, and so on.^{1–3} These applications are based on photoinduced generation of electrons and holes at the TiO₂ surface, which are consequently converted into excitons in quantum states near the surface (surface states) after energy relaxation. In this process, fast e–h recombination takes place to form the luminescent exciton states, and the charge carriers are not so efficiently transferred to substrate for redox reaction. Thus, it has been interesting subject how the efficient polarization and retarded

recombination of the electron and hole (e–h) pairs can be achieved in the surface states.

The exciton dynamics of semiconductor nanoparticles are known to be controlled by two factors.^{4,5} One is to increase specific surface area by reducing the size of the nanoparticles. As the particle size (diameter) is smaller than the thickness of space charge layer, the surface area becomes larger, and the charge separation becomes effective to retard the e–h recombination. However, the ultrafine nanoparticles have a tendency to agglomerate into larger particles in the practical use, resulting in adverse effect on the exciton dynamics. Thus, increasing the surface area by reducing the particle size is limited, and the other important factor to control the exciton dynamics is to improve the surface state characteristics such as surface state density and electron/hole trapping kinetics by decreasing the degree of overlap of the electron and hole wave functions through modification of the surface structures. Therefore, there have been many attempts to modify the surface structures of TiO₂ nanoparticles to improve behavior of the surface states with the aim to design of highly efficient photocatalyst.

One of the surface modifications has been usually carried out by incorporation of TiO₂ quantumdots (QDs) with some supporters such as zeolites and Vycro glass,^{6–9} but it causes reduction of optical cross section so that the improvement of photocatalytic activities are limited. Alternatively, synthesis of low-dimensional single-crystalline TiO₂ nanostructures as

^a Molecular/Nano Photochemistry & Photonics Lab, Department of Chemistry, Chungnam National University, Daejeon, 305-764, Korea. E-mail: mjyoon@cnu.ac.kr

^b Advanced Materials Division, Korea Research Institute of Chemical Technology (KRICT), P. O. BOX 107, Yuseong, Daejeon, Korea

^c Department of Applied Physics, Osaka University, Suita, Osaka 565-0871, Japan

^d Present address: Graduate School of Materials Science, Nara Institute of Science and Technology (NAIST), Ikoma City, Nara Prefecture 630-0192

† Electronic supplementary information (ESI) available: LSCM-coupled ps-time-resolved PL system and movie of blinking PL of TiO₂ NDs. See DOI: 10.1039/b812361f

nanotubes (NTs)^{10–12} and nanodiscs (NDs)¹³ has been one of the most promising options to control the surface states and exciton dynamics to improve the photocatalytic activity as the TiO₂ NTs and TiO₂ NDs have been applied to develop highly efficient photocatalysts and dye-sensitized solar cells.^{10,13} In the nanostructures, the photoinduced electron transfer is speculated to be facilitated through the surface layer because of high aspect ratio and surface area reducing inter-crystalline contacts of TiO₂. Nevertheless, there are few systematic studies to clarify the surface state behaviors of the TiO₂ nanostructures with regard to the exciton dynamics, particularly interfacial electron transfer dynamics.

The exciton dynamics of the nanoparticles have been mostly investigated using laser spectroscopic techniques including diffuse reflectance transient absorption spectroscopy^{14–16} and time-resolved PL spectroscopy^{17,18} from femtosecond to millisecond time scale as well as steady state PL spectroscopy. However, the conventional techniques are based on ensemble-average of the spectral properties which are very sensitive to the particle size, morphology and surface compositions of the nanoparticles.^{14,15,19} Practically, TiO₂ nanoparticles have inhomogeneity of size and morphology distributions, and the ensemble-averaged spectral techniques have limited in clear understanding of the surface-exciton dynamics as well as the optical properties of the TiO₂ nanoparticles. Therefore, in order to solve these problems, it is necessary to probe individual nanoparticle behaviors hidden within the uncorrelated ensemble systems by using single nanoparticle spectroscopic techniques similar to single molecule spectroscopy.

During the last decade, there have been some applications of the single nanoparticle spectroscopy to study the surface state behaviors of single semiconductor QDs such as ZnS-overcoated CdS, CdSe and CdTe,^{20–26} InGaAs/GaAs²⁷ and Y₂O₃:Eu³⁺ QDs.²⁸ Such investigations have yielded the statistics of photoluminescence (PL) luminescence switching events between bright (“on”) and dark (“off”) state (blinking),²⁰ and there have been various models proposed for blinking mechanisms in the QDs. A commonly accepted model of the blinking events in the II–VI colloidal QDs was firstly suggested by Efros and Rosen,²⁹ which is based on a long-lived trap hypothesis that PL is quenched by trapping of the exciton pair in the long-lived surrounding matrix (*e.g.* ZnS) and consequent Auger ionization. In the ionized QDs, the exciton pair can be recombined by an ultrafast radiationless Auger process (~ 1 ps).²³ That is, the PL switching events are connected with the electron transitions from the QD to the long-lived trap site. This mechanism has been supported by several experiments^{30,31} and theoretical calculations.²⁵ More advanced explanations have been attempted to explain the power law distribution of “off” times using a wide range of exponentially distributed ionization-recombination rates, switched randomly after each electron transition between the QD states and the surrounding multiple electron traps.³² The electron transfer event switching the PL intensity was proposed to happen only when the excited state and trap state are in resonance, providing a concept of a slow diffusive coordinate which explains the large difference between excitation-relaxation times of electronic states of the QD and the blinking times.³³ This proposition is based on assumption of

an existence of a single electron trap state, and this model was improved by Tang and Marcus³⁴ and Margolin *et al.*³⁵ explaining the PL blinking caused by three dimensional hopping diffusion of the photoejected electron into the surrounding trapping media. The ionized QD stays “off”, while the QD stays “on” as long as the electron diffusing with the hole trapped. However, this model cannot explain the escape of the trapped electron such as the interfacial electron transfer. Thus, Frantsuzov and Marcus³⁶ proposed alternative model without the long-lived trap hypothesis, and Pelton and Marcus *et al.* verified it by characterizing the blinking fluctuations of ZnS/CdSe QDs over time scales from millicoseconds to seconds.³⁷ According to their model, the PL intermittency of QD is caused by large variations of the radiationless relaxation rates of the excited electronic state to the ground state *via* the hole trap states induced by an Auger-assisted hole trapping to the deep surface states, which is accompanied by the simultaneous electron excitation to the higher electronic states beyond the conduction band. They found that the PL blinking is controlled by diffusion of the energies of electron or hole trap states as a function of the nuclear coordinates of the system. Nevertheless, this blinking mechanism has not been tested yet in the absence of the surrounding matrix (ZnS) which would act as a long-lived trap. Thus, it would be interesting to verify this mechanism by using the naked QDs. However, usually the exciton recombination in the naked QDs is too fast to exhibit the PL intermittency, and it is necessary to modify the QDs into low dimensional nanostructures. Very recently, Glennon *et al.*^{38,39} observed PL blinking of one dimensional CdSe quantum wires, the mechanism of which was suggested to be different from that commonly explained for the PL blinking of semiconductor QDs, presenting a simple surface-trap-filling model based on the dynamic, transient filling of surface-trap sites by excitons and the emptying the occupied trap sites.

Herein, in order to unequivocally understand the surface-modification effects on exciton dynamics of the TiO₂ nanoparticles, the single nanoparticle PL spectroscopy coupled with laser scanning confocal microscopy (LSCM) was applied to the two dimensional TiO₂ NDs without any additional surrounding matrix, which are expected to have different surface characters than those of TiO₂ QDs. We observed wide-field blinking PL images of the single TiO₂ NDs for the first time, and analyzed their blinking kinetics. The PL emission spectra of the individual ND and their temporal behaviors were also measured. These results suggest that the PL blinking of TiO₂ NDs is due to slow interfacial electron transfer to the surface trap sites with simultaneous Auger-assisted hole trapping in the multiple surface states, similarly to the diffusive coordinate model,³⁶ implying the existence of inherent long-lived trap states to retard the radiationless exciton recombination in the TiO₂ NDs.

2. Materials and methods

TiO₂ NDs were synthesized by sol-gel method through formation of liposome-TiO₂ nanocomposites using egg-lecithin lipid as a template as previously established method.¹³ The crystalline phase of the produced materials were identified by X-ray diffraction patterns of the sample recorded on Rigaku

Rotaflex diffractometer (Model No. D/MAX-2200 Ultima/PC, rotating Cu K α target, 3 kW X-ray and set to 40 kV and 40 mA). The morphology of the synthesized materials was examined by transmission electron microscope (TEM) (JEOL JEM-2010, Japan) and atomic force microscope (AFM) (NanoScopeIIIa, DI, USA). Samples for TEM measurement were prepared by dip coating formvar/carbon film Cu grids with the nanocolloidal solution obtained by sonicating the produced powder material in ethanol. On the other hand, AFM images were obtained by tapping mode for the samples prepared by spin casting (3000 rpm) a solution (~ 500 ppm) of the nanostructures onto a glass or quartz cover slip which was thoroughly cleaned by sequential sonication in acetone, methanol, deionized water, aqueous solution (10% by volume) and deionized water, respectively, each for 10 min and dried in a jet of nitrogen gas. As TiO $_2$ QD nanoparticles, Degussa P-25 was used as purchased from Degussa Co. The samples prepared for the AFM measurements were also used to measure the single nanoparticle and ensemble-averaged photoluminescence (PL) properties. The ensemble-averaged PL spectral measurements were taken on a SLM-Aminco 4800 spectrofluorometer by diffuse reflectance method.

The PL measurements of the single TiO $_2$ -NDs or TiO $_2$ QDs were performed by using LSCM-coupled ps-time-resolved PL system⁴⁰ (ESI S-Fig. 1 \dagger) at room temperature. The sample-coated cover slide glass on a scanning piezo-electric X–Y stage (Physik Instrumente, P517.3CL) was illuminated with 405 nm light ($\sim 10 \mu\text{W cm}^{-2}$) from CW diode laser (NEO ARK, LDT-4005) or second harmonic generated self-mode-locked Ti:sapphire laser (Coherent model Mira 900) (390 nm) pumped by a Nd:YVO $_4$ laser (Coherent Verdi diode pumped laser) (200 fs pulse width with repetition rate of 76 MHz) for PL images, steady-state and time-resolved spectra measurements, respectively. This light was passing through the single mode optic fiber and then incident on the back of a 100×1.3 NA oil immersion objective lens (Carl Zeiss Plan-NEOfluor). The PL signals were collected through an inverted confocal scanning microscope (Carl Zeiss Axiovert 200). The emission was isolated from Rayleigh scattering by a combination of filters, an excitation filter BP 395–440, a dichoric filter FT 460 and an emission filter LP 470 (Carl Zeiss).

The blinking PL images of the single TiO $_2$ NDs were obtained through detection of epiluminescence over a focused laser spot of ~ 300 nm diameter by using a liquid-nitrogen-cooled intensified charge-coupled device (CCD) detector (Princeton Instruments VersArray) *via* single-photon counting avalanche photodiode (Perkin-Elmer SPCM-AQR-13FC) with wide-field excitation in a similar way to the single molecule PL detection.⁴¹ The chip of the CCD has a total active area of 12.3×12.3 mm divided into 512×512 pixels (size: $24 \times 24 \mu\text{m}$), which was operated at -110 °C. The blinking events were collected every 50 ms exposure per frame, respectively. One pixel represents an area of 240×240 nm on the sample-coated cover glass. Wide-field images were acquired with the software WinSpec (Princeton Instruments).

PL spectra of a single ND image, which was selected from several NDs obtained by confocal method through raster-scanning of the sample-coated slide glass over the inverted microscope, were recorded by a polychromator (Acton

Research, Spectra Pro 300i) with a charge coupled device (CCD) camera (Roper Scientific, PI-MAX-1024HG18) *via* optical fiber. The spectra were measured continuously with accumulation of emissive photons within 200 ms per spectrum at room temperature. The raster-scanning PL image of the single NDs were collected by the same objective lens and focused on single-photon counting avalanche photodiode (Perkin-Elmer SPCM-AQR-15) after passing a polarization beam splitter. Scattered light was removed holographic notch filter (Kaiser, HNPF-405.0-1.0). Electronic properties of TiO $_2$ surface are known to depend on excitation intensity,^{16,42} and the high power of the excitation light makes the surface photochemistry and exciton dynamics so complicated that the data obtained with high excitation intensity would be misjudged. Therefore, it is necessary to acquire the single nanoparticle spectral data with the lowest power of the excitation light as far as allowed. The excitation wavelength was 390 nm and its intensity was $10 \mu\text{W cm}^{-2}$.

The PL decay times of a single ND were measured by time-correlated single photon-counting (TCSPC) system (Edinburgh Instruments) with time resolution of 20 ps at room temperature. The start signal was collected through the multi mode optic fiber from the confocal microscope and the signal was stopped by synchronization of the Ti:sapphire laser pulse which was passed through a pulse picker at one-half of the laser repetition rate.

3. Results and discussion

Fig. 1(A) and (B) show TEM and AFM images of spherical TiO $_2$ NDs, respectively, from which the TiO $_2$ NDs were identified to be anatase crystalline (as seen from the well-defined SAED and 0.35 nm lattice spacing) with the average diameter of 9 nm and central height of ~ 2 nm as determined from the cross sectional analysis of the AFM images (ESI S-Fig. 2 \dagger).¹³ Fig. 1C shows the ensemble-averaged diffuse reflectance PL emission and excitation spectra of the TiO $_2$ NDs deposited on the slide glass, exhibiting broad emission band in the range from 400 nm to 650 nm as observed previously.^{12,13} This was attributed to e–h recombination at different surface-states because the PL excitation band was clearly observed at 405 nm corresponding to the weakly observed surface state absorption with indirect band gap energy 3.03 eV,¹³ and the PL images and spectral data of single NDs were acquired by excitation at 390 or 405 nm.

The PL image of the single NDs deposited on the quartz slide glass (as seen on the AFM image) was obtained by wide-field excitation with 390 nm light and analyzed using threshold criterion. The excitation light intensity was observed to differ not more than 20% in the whole viewing field and less than 10% in the one-quarter portion of the image selected here for observation. The background noise amplitude originated from CCD detector was subtracted from the total photon counts in each pixel. This resulted in mean noise amplitude ± 40 counts independent of the position, but slightly dependent on the exposure time. The threshold was set to 150 counts which are about three times of the mean noise amplitude. With this procedure, we collect truly representative counts of all emission signals from the nanostructure particles in the field of

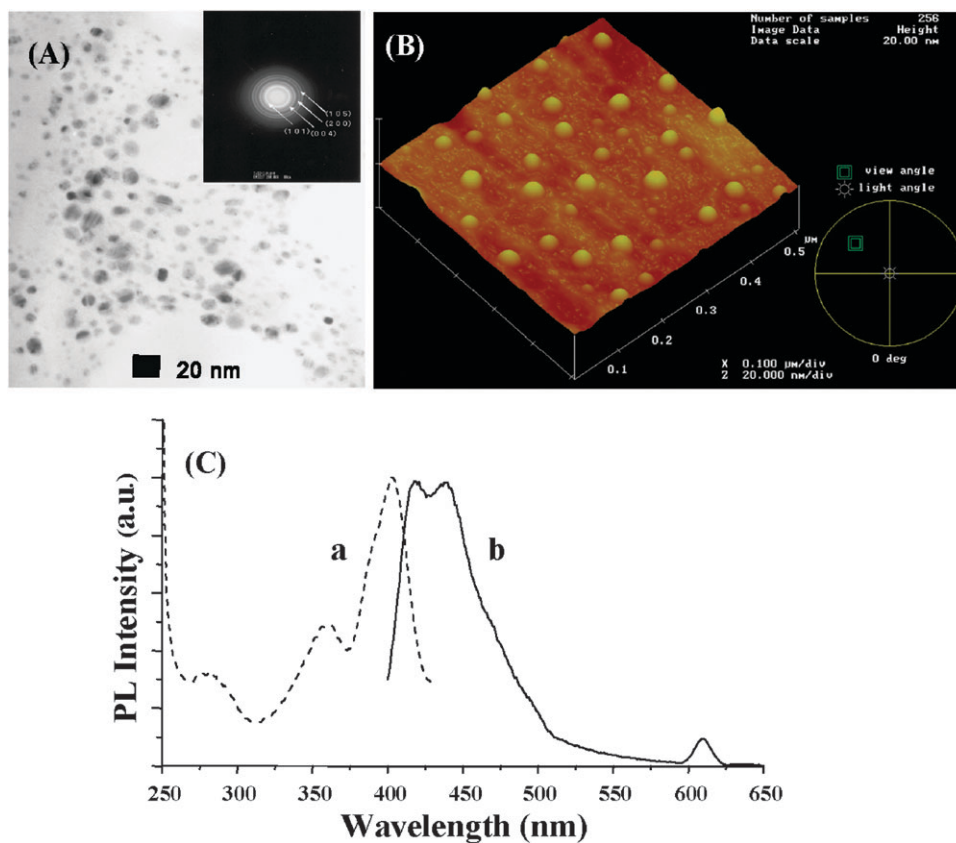


Fig. 1 (A) TEM images of TiO₂ NDs showing anatase SAED (Insert). (B) AFM images of TiO₂ NDs on quartz slide glass measured by tapping mode. The average height of the TiO₂ ND is ~ 2.0 nm as determined from a cross-sectional analysis (ESI S-Fig. 2†) of the AFM image. (C) The ensemble-averaged PL excitation (a) and emission (b) spectra of TiO₂ NDs measured at ambient temperature. The excitation wavelength for the emission spectrum was 360 nm, and the emission wavelength for the excitation spectrum was 440 nm.

view in every 50 ms binning time. The measured wide-field PL images of TiO₂ NDs display emissive spots as shown in Fig. 2(A). The brightest big spot is bulk emission of many ND particles included in the focused laser spot within ~ 300 nm diffraction limit. Most of other small spots keep a certain level of PL emission but periodically displays blinking (as seen in the ESI†) in the way which the emission is quenched to form a darker “off-state” and returns to the original intensity after a brief time to resume the bright emissive “on-state”. The blinking persisted during minutes of observation, which did not appear to photobleach or change color. These blinking behaviors appear to be generally comparable to those observed from ZnS-coated CdSe QDs,²³ InGaAs/GaAs²⁷ and Y₂O₂S:Eu³⁺ QDs²⁸ as well as ITO glass-adsorbed single molecules,⁴¹ which may be caused by repetitive trapping and detrapping of the excitons in the matrix like ZnS acting as a long-lived trap site, as explained by many models of the long-lived trap hypothesis.^{29–35} However, TiO₂ NDs do not have the surrounding matrix, and their blinking behaviors may be related to existence of inherent surface trap sites which trap the photogenerated electron *via* interfacial electron transfer. Thus, the blinking behavior of TiO₂ NDs would be better explained by combination of a model without the long-lived trap hypothesis as proposed by Marcus group,^{36,37} and the simple surface-trap-filing model proposed for the CdSe nanowire.^{38,39}

The time-dependent PL intensities of one representative spot are shown in Fig. 2(B–(a)). Similar blinking behaviors were observed from over 80% of 85 selected spots which show rapid fluctuation in the PL intensity. Then, it is noteworthy that very weak PL intensities with little fluctuation were observed for TiO₂ QD nanoparticles under the same experimental conditions as those for the TiO₂ NDs (Fig. 2(B–(b))), indicating that the surface exciton dynamics of TiO₂ QD are very different from those of TiO₂ ND.

To understand the blinking PL behaviors in detail, the luminescent blinking kinetics of one represented spot were examined by determining the average lifetimes of the “on-state” and “off-state” through analyzing the time distributions with a method similar to that previously used to analyze blinking due to interfacial electron transfer in self-assembled single molecules on ITO glass.⁴³ Taking the PL trace shown in Fig. 2B–(a) as an example, a histogram of the PL intensities of a single TiO₂ ND was built up as shown in Fig. 3A, which shows clearly that there are two states with two different levels of PL: a state with an average intensity of approximately 175 counts/50 ms, which corresponds to the background PL (the “off” state); and a state with an average intensity of approximately 235 counts/50 ms, which is equal to a typical PL level above the background for a single TiO₂ ND under our experimental conditions (the “on” state). On the other hand, the histogram of the TiO₂ QD built up by taking PL trace shown in

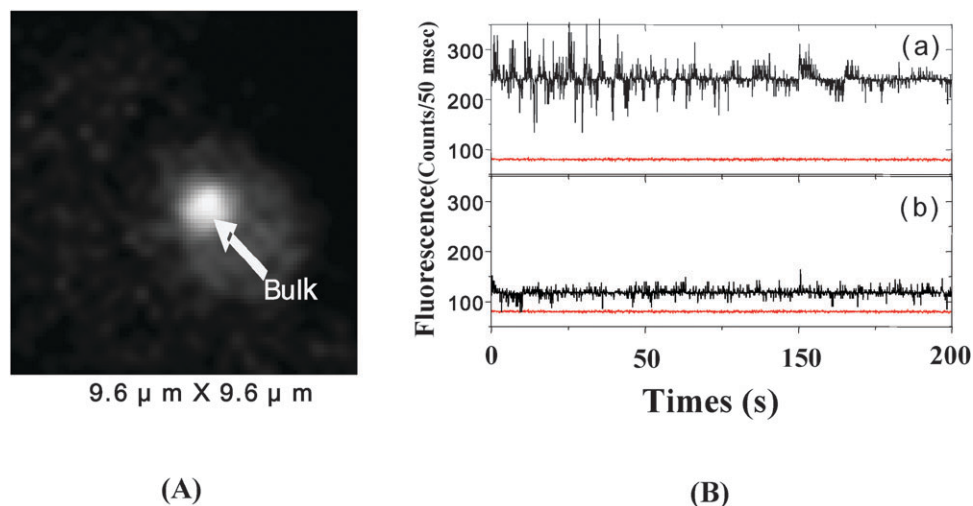


Fig. 2 (A) Wide-field photoluminescence image of TiO₂ NDs measured upon excitation of 390 nm on inverted laser scanning microscope (40 × 40 pixels). The 390 nm excitation intensity was 10 μW cm⁻². For this image, an oil immersion objective (1.3 × 100 NA) was used. The image was collected in a zoom time frame (50 ms). (B) Time-dependent trajectories of PL intensities for one representative single TiO₂ ND (a) and TiO₂ QD (b). The bottom traces (red color) are the non-luminescent background noise levels measured from the slide glass without TiO₂ nanoparticles.

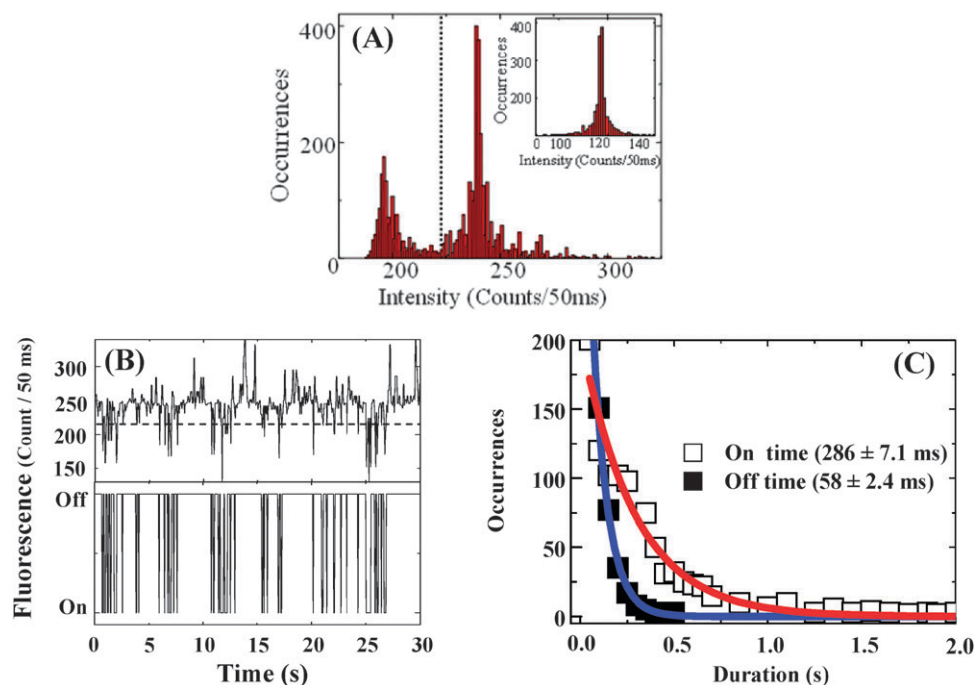


Fig. 3 (A) A PL intensity histogram of the trace for TiO₂ ND as obtained from Fig. 2(B-a). The insert shows the intensity histogram of the trace for TiO₂ QD as obtained from Fig. 2(B-b); (B) A section of the trace and the same section rounded to on and off states; (C) A histogram as a function of occurrences vs. the on and off time durations showing single exponential fit.

Fig. 2B–(b) shows only one luminescent state, indicating again that PL blinking is negligible for TiO₂ QD (inset in Fig. 3A). The luminescent blinking kinetics of a single TiO₂ ND were analyzed by rounding off the trace using a cutoff point a value of 220 counts/50 ms; the single ND is assigned to either the “on” or the “off” state at each point in the trace (Fig. 3B) as the PL is greater or less than this cutoff. The duration of the on and off times were counted and histogrammed as occurrences vs. duration time, and the histograms

were found to fit with single-exponential curves (Fig. 3C), indicating that blinking behavior is related to geminate recombination of e–h pairs induced even by the weak excitation (10 μW). From the single exponential histograms, the average lifetimes of the on and off states were determined; the average lifetimes of the on-state (τ_{on}) and off-state (τ_{off}) are ~286 ms and ~58 ms, respectively. The “off”-state lifetime is too long to be accounted for by radiationless relaxation of e–h pairs to the surface states in competition

with e-h recombination,^{12,13,16} and the occurrence of “off” state is related to long time separation of the excitons in the surface states and consequent interfacial electron transfer, supporting existence of inherent surface trap sites. Moreover, the single exponential kinetics strongly implies that the nanostructure system is fixed and well behaved. Thus, the blinking is due to a single process, interfacial electron transfer to the ${}_{4}\text{Ti}^{4+}\text{-OH}$ surface trap sites with the simultaneous Auger-assisted hole trapping by alternative trapping and detrapping of excitons through the multiple surface states similarly to the diffusive coordinate model proposed by Frantsuzov and Marcus.³⁶ In competition with the radiative exciton-recombination, the hole is captured into a deep surface state while the electron diffuse to the higher electronic energy through the surface states (Auger process), forming “off”-state until the electron returns and the nanostructures resume “on” with emission. If this is the case, the density of surface states of TiO_2 NDs is much higher than those of TiO_2 QDs so that the lifetime of surface-trapped electron is longer. Actually lifetime of the surface-trapped electron of TiO_2 QDs is much shorter (30 ps)⁴⁴ than that of TiO_2 NDs (~ 8 ns).¹³

In order to check these speculations, it is necessary to examine the surface states of the TiO_2 NDs, and the PL emission spectra and the PL decay times of the representative single TiO_2 ND selected from the raster scanned PL images (Fig. 4A) were measured at room temperature. The PL emission spectra of the single TiO_2 ND of different sizes are shown in Fig. 4B. As the ND sizes decreased, the intensities of the surface emission bands were observed to decrease without any band shift, indicating that the quantum confinement effect is not as important in the nanostructures as in the QDs. Generally emission bands observed around 520–600 nm are relatively stronger than 470 nm. This trend is opposite against that observed from the bulk emission. Anyhow the overall spectral bands seem to be still broadened, even though the inhomogeneity of the size distribution is ruled out in this work. This broadening must be originated from energy diffusion of the multiple surface states involved in the exciton dynamics on the surface of the TiO_2 nanostructures.^{36,37} In fact, the PL emission band was assumed to have Gaussian and Lorentzian line shapes and could be analyzed to be composed of four different emission bands at 470 nm (2.64 eV), 520 nm (2.40 eV), 550 nm (2.25 eV) and 650 nm (1.91 eV) (Fig. 4C), by using the nonlinear least square method. On the basis of the transition energy diagrams of TiO_2 particles calculated by Daude *et al.*,⁴⁵ the first three higher energy bands are attributed to the shallow and deep surface states near the ${}_{4}\text{Ti}^{4+}\text{-OH}$ surface, while the 650 nm band is attributed to the defect states originated from ${}_{6}\text{Ti}^{3+}\text{-OH}$, a coordinatively unsaturated ion (*cui*) as reported previously.^{12,13,46} Interestingly, the intensity of the 650 nm band is relatively weaker than those of the higher energy bands while 520–550 nm band is much stronger as compared to 470 nm band observed from the bulk emission. This indicates that the population of the ${}_{4}\text{Ti}^{4+}\text{-OH}$ sites and the deep exciton state is much higher than that of *cui* sites in the nanostructure than in TiO_2 QDs. This is consistent with the previous reports of XPS analysis results.^{12,13} This result is opposite against the observation that

the population of *cui* sites is rather higher than that of ${}_{4}\text{Ti}^{4+}\text{-O}$ sites in the TiO_2 QDs³³ which do not display the PL blinking. There are two types of hydroxide ions present at the surface of TiO_2 . One is basic and attached to one Ti^{4+} , which acts as the hole trap surface sites, and the other is acidic and bridges two Ti^{4+} which acts as the electron trap surface sites.^{47,48} Interestingly, the IR band of second type OH was more strongly observed from TiO_2 NDs as compared to that observed from TiO_2 QDs,¹³ implying that the NDs should have a larger number of dangling ${}_{4}\text{Ti}^{4+}\text{-OH}$, or ${}_{4}\text{Ti}^{4+}\text{-O-}_{4}\text{Ti}^{4+}$ bonds as expected from the significantly larger specific surface area of the NDs in comparison to the QDs of similar diameters¹³ as in the case of CdSe nanowires.³⁸ Therefore, these results suggest that the peculiar surface structure of TiO_2 NDs plays an important role in the PL blinking, being consistent with the presence of multiple surface states and many surface trap sites required for the diffusive coordinate model proposed by Frantsuzov and Marcus³⁶ and the simple surface-trap-filling model.³⁹

To confirm the multiple surface states with respect to the e-h recombination dynamics, the PL decay times of the selected single TiO_2 ND were measured by monitoring different emission bands (470 nm and 550 nm) at the blinking “on-time” duration to rule out a possible detection of the time-averaged multi-exponential decays. The decays were analyzed to be single or bi-exponential in contrast to multi-exponential decay observed for the ensemble-averaged emission attributed to inhomogeneous distribution of particle size.^{11,12} The decay times are summarized in Table 1. Decay time of 470 nm emission is 470 ps. The 1.0 ns component is also observed with another longest component (7.58 ns) for decay of 550 nm emission. This analysis indicates that there are three surface states having three different decay times, 470 ps, 1.0 ns and 7.58 ns, which correspond to the decay times of 470 nm, 520 nm and 550 nm emission, respectively, as analyzed from the PL spectra. Unfortunately, the 650 nm emission band was too weak to be monitored for the decay time measurement. It is interesting to note that the long decay times of the surface emission at 550 nm were not observed from TiO_2 QDs in spite of similar quantum yields.^{11,12} The long decay time of the deep surface emission means that the e-h recombination is relatively slower in the TiO_2 nanostructures than in the TiO_2 QDs, and the electron or hole can be easily escaped from the deep surface states in competition with the e-h recombination. Actually, in the TiO_2 QDs, the e-h recombination is quite rapid with a majority of recombination time within 50 ps,^{18,44} and the e-h separation is more or less prohibited so that the forward interfacial electron transfer is not so feasible as in the nanostructure. This may be the reason why little PL blinking is observed from the TiO_2 QDs. Therefore, we believe that the PL blinking of the TiO_2 NDs results from the Auger-assisted interfacial electron transfer to the ${}_{4}\text{Ti}^{4+}\text{-OH}$ trap sites from the deep surface state.²⁵

Based on the above experimental results, we propose a model for the PL blinking mechanism by modifying the diffusive coordinate model proposed by Frantsuzov and Marcus³⁶ and the simple surface-trap-filling model³⁹ as shown in Fig. 5A. Upon CW laser excitation a certain number of free

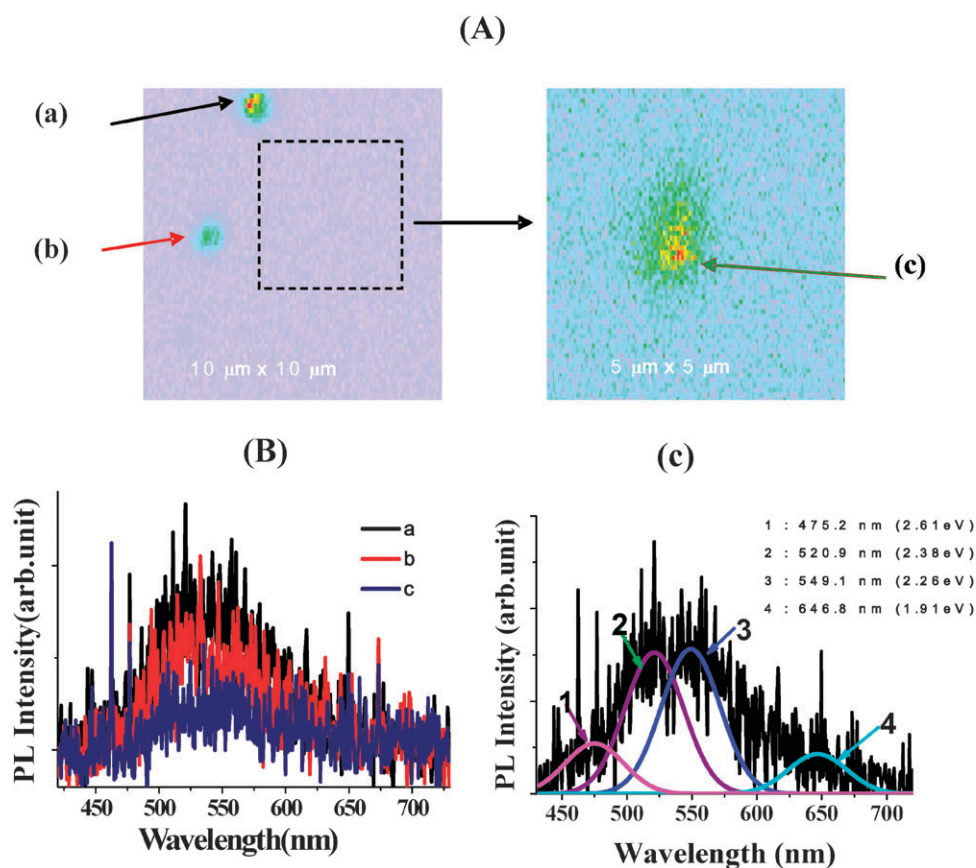


Fig. 4 (A) Raster scanned PL image of four single TiO₂ NDs of different sizes. (B) PL spectra of the selected three spots pointed in (A) and the bulk PL spectrum (blue curve) measured from the laser focal spot as shown in Fig. 3. (C) PL spectrum analyzed by using nonlinear least squares method based on the Gaussian and Lorentzian line shapes.

Table 1 PL decay times of single TiO₂ NDs measured at different emission wavelengths

λ_{em}	τ_1/ns	τ_2/ns	χ^2
470 nm	1.03 (51.1%)	0.47 (48.9%)	1.06
550 nm	7.58 (63.3%)	1.00 (36.7%)	1.09

e-h pairs with delocalized wave functions are generated in the conduction band and valence band in the neutral nanostructures, forming ground bulk state (GS), and after radiationless relaxation they are mostly trapped in the surface states, and bounded to the deep surface states (ES*) releasing luminescence through radiative recombination processes, forming “on” state. Simultaneously, in the course of relaxation processes, one of those excitons annihilates without emitting a photon and its energy can be borrowed by the second exciton (Auger process). Thus, the electron detraps to the localized shallow surface states (SS*) and consequently diffuses into the higher electronic states, the energy of which may be controlled by the surface trap site to form the surface trap states (ST) with the hole trapped in the deep surface state, forming non-luminescent “off” state of the ionized (or e-h polarized) nanostructures. The “off” state remains until the electron returns back to the hole trap state for the radiationless recombination with the hole to form the neutral ground

state which resumes the luminescence by photoexcitation. In this process, the interfacial electron transfer is supposed to be much slower than the pure Auger-assisted electron or hole transfer. In fact, recent transient absorption studies of nanocrystalline TiO₂ films identified the holes captured at the surface in less than 100 fs which is much shorter than electron trapping and the Auger-assisted electron detrapping,¹⁶ supporting the interfacial electron transfer as the rate determining process for the Auger process. Thus, the PL blinking kinetics and mechanism can be determined mostly in terms of the interfacial electron transfer and surface state-trapping of electrons. The switcher of PL with the electron trapping and interfacial electron transfer to the surface trap site is described in terms of energy transformation as shown in Fig. 5B.

In accordance with the diagram shown in Fig. 7B, the rate of the back electron transfer (k_{bet}) corresponding to trapping into the surface states from the surface trap site is simply the inverse of the average lifetimes of the off-state.

$$\frac{1}{\tau_{\text{off}}} = k_{\text{bet}} \quad (1)$$

On the other hand, the decay rate of the on-state ($1/\tau_{\text{on}}$) via the electron escape doorways also depends on the excitation rate (k_{exc}) and luminescent decay rate (k_r) of the exciton states

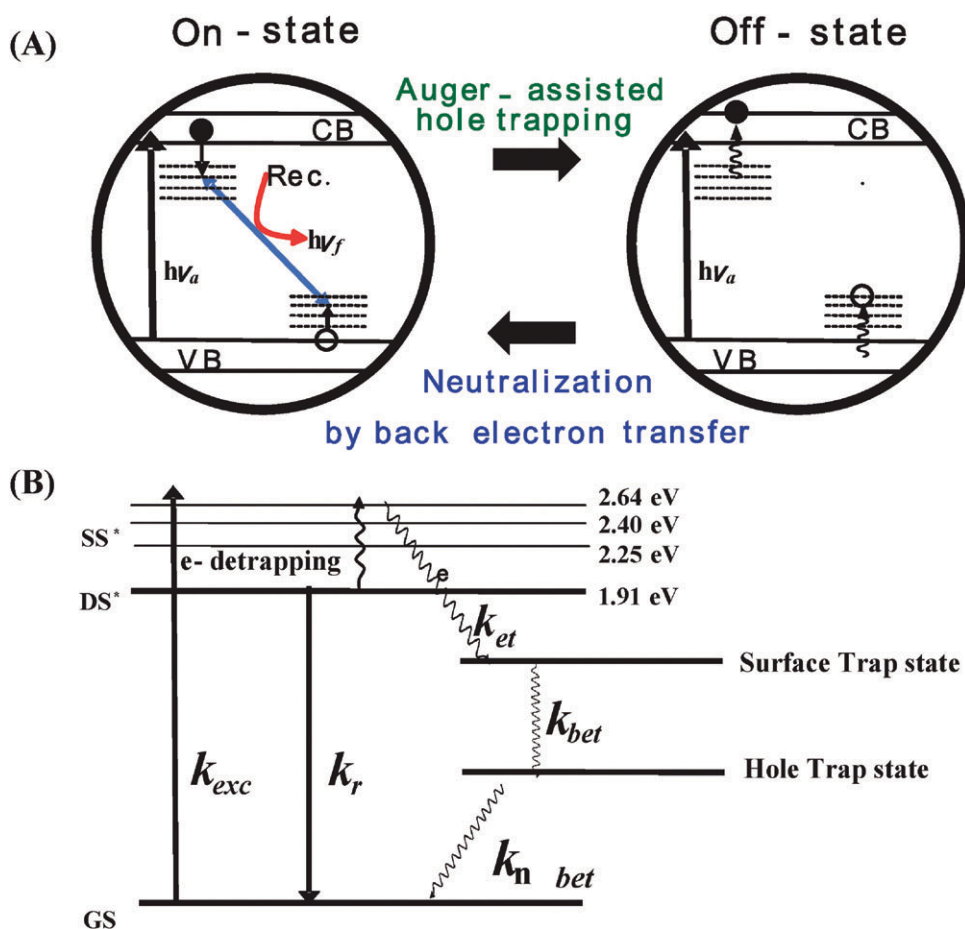


Fig. 5 (A) Ionization/neutralization process through electron trapping (tr) and detrapping (dep) in TiO₂ nanostructures under laser illumination, forming PL on-state and off-state. T and Rec stands for surface trap-site and recombination, respectively. (B) Energy transformation model for the switcher of PL with the electron detrapping and interfacial electron transfer to the surface trap state for TiO₂ nanostructures whose PL displays blinking behavior. From this model, rates of interfacial electron transfer to the surface trap site forming surface trap state (k_{et}) and back electron transfer (k_{bet}) to the hole trap state were determined. Once the electron is transferred back to the hole trap state, very fast radiationless relaxation (k_n) would take place.

which correspond to the e–h recombination rate, as well as the rate of interfacial electron transfer (k_{et}).²⁵

$$\frac{1}{\tau_{on}} = k_{exc} \frac{k_{et}}{k_r + k_{et} + k_{exc}}. \quad (2)$$

Thus, once τ_{on} and τ_{off} have been determined, the rates of forward and backward electron transfer can be readily determined by using eqn (1) and (2). Taking power ($10 \mu\text{W cm}^{-2}$) of 390 nm laser and absorption cross sections of ND, $\sigma_{ND} = 7.9 \times 10^{-13} \text{ cm}^2$ based on the average sizes of each nanostructure determined from TEM images shown in Fig. 2, we estimate $k_{exc} = 15.4 \text{ s}^{-1}$. Assuming that k_r is the inverse of average luminescent decay time of the surface emission at 550 nm, it was calculated to be $1.9 \times 10^8 \text{ s}^{-1}$. With these values and the average lifetimes of on-state and off-state for the single NDs the rates of the forward and backward interfacial electron transfer are calculated as shown in Table 2. Interestingly the forward interfacial electron transfer rate is more or less comparable ($5.5 \times 10^7 \text{ s}^{-1}$) to the e–h recombination rate corresponding to luminescent relaxation (k_r) whereas the backward electron transfer rate constant is quite slow as compared to the forward electron transfer. This indicates that the trapping depth of NDs is bigger than that of QDs, probably

Table 2 Average on-time (τ_{on}) and off-time (τ_{off}), calculated rates of interfacial electron transfer and back electron transfer in TiO₂ nanodiscs

τ_{on}/ms	τ_{off}/ms	k_{et}/s^{-1}	k_{bet}/s^{-1}
286 ± 7.1	58 ± 2.4	$(5.5 \pm 0.1) \times 10^7$	17.2 ± 0.6

because the density of $4\text{Ti}^{4+}\text{-OH}$ sites is higher in NDs than in QDs as discussed above. From these results, we are convinced that electron transfer to the proximate substrate would be highly efficient in the surface-modified TiO₂ nanoparticles, TiO₂ NDs as compared to the TiO₂ QDs which allow the efficient interfacial electron transfer only if electron donor or acceptor molecules are strongly associated with particle surface.⁴⁹ Thus, formation of the long-lived (milliseconds) e–h polarized state in TiO₂ NDs is confirmed to be so feasible as the highly efficient photocatalytic activities was obtained as previously reported.¹³

4. Conclusion

Blinking PL images were observed for the first time from single TiO₂ NDs upon illumination at surface absorption wavelength

around 400 nm in contrast to little PL blinking of TiO₂ QDs. The histograms of duration of the on and off states fit single exponential to determine the average lifetimes of on-state and off-state which are very long as compared to the radiative and non-radiative relaxation times, indicating a single process, *i.e.* interfacial electron transfer, is involved in the blinking. The PL emission spectra and emission decay times of the individual nanostructure demonstrated that four surface states are involved in slow rate of e–h recombination, implying that the blinking mechanism of TiO₂ NDs fits with a simple model modified from the diffusive coordinative model and surface-trap-filling model. Based on this blinking model, the rate of interfacial electron transfer and back electron transfer was determined to be slow enough to keep the polarization of e–h pairs at surface for efficient photocatalysis and photovoltaic activities. The present methodology and results may be applicable to obtain surface exciton dynamics of various photoelectronic semiconductor nanostructures.

Acknowledgements

This work has been financially supported by the Korea Science and Engineering Foundation through special basic science project (Grant R01-2004-000-10446-0), Joint Research Project under the Korea-Japan Basic Scientific Corporation Program (KOSEF F01-2004-000-10024-0), the Korea Research Foundation (KRF C00340) and “Development of Advanced Scientific Instrument” program funded by the Ministry of Education, Science and Technology.

References

- M. Yoon, J. A. Chang, Y. Kim, J. R. Choi, K. Kim and S. J. Lee, *J. Phys. Chem. B*, 2001, **105**, 2539.
- S. Khan, M. Al-Shahry and W. Ingler, *Science*, 2002, **297**, 2243.
- Q. Li, R. C. Xie, Y. W. Li, E. A. Mintz and J. K. Shang, *Environ. Sci. Technol.*, 2007, **41**, 5050.
- W. Chen, *Fluorescence*, in *Handbook of Nanostructured Materials and Nanotechnology*, ed. H. S. Nalwa, Academic Press, New York, USA, 2000, ch. 5, vol. 4.
- Y. Wang and N. Herron, *J. Phys. Chem.*, 1991, **95**, 525.
- S. Corrent, G. Cosa, J. C. Scaiano, M. S. Galletero, M. Alvaro and H. Garcia, *Chem. Mater.*, 2001, **13**, 715.
- S. Anandan and M. Yoon, *J. Photochem. Photobiol., C*, 2003, **4**, 5.
- M. Anpo, N. Aikawa and Y. Kubokawa, *J. Phys. Chem.*, 1985, **89**, 5017.
- R. W. Matthews, *J. Phys. Chem.*, 1988, **92**, 6853.
- M. Adachi, Y. Murata, M. Harada and S. Yoshikawa, *Chem. Lett.*, 2000, 942.
- Q. Chen, G. H. Du, S. Zhang and L.-M. Peng, *Acta Crystallogr., Sect. B*, 2002, **58**, 587.
- J. H. Jang, K. S. Jeon, T. S. Park, K. W. Lee and M. Yoon, *J. Chin. Chem. Soc.*, 2006, **53**, 123.
- M. Yoon, M. Seo, C. Jeong, J. H. Jang and K. S. Jeon, *Chem. Mater.*, 2005, **17**, 6069.
- A. Furube, T. Asahi, H. Masuhara, H. Yamashita and M. Anpo, *Chem. Lett.*, 1997, 735.
- A. Furube, T. Asahi, H. Masuhara, H. Yamashita and M. Anpo, *J. Phys. Chem. B*, 1999, **103**, 3120.
- T. Yoshihara, R. Katoh, A. Furube, Y. Tamaki, M. Murai, K. Hara, S. Murata, H. Arakawa and M. Tachiya, *J. Phys. Chem. B*, 2004, **108**, 3817.
- A. Amtout and R. Leoneli, *Solid State Commun.*, 1992, **84**, 349.
- K. Fujihara, S. Izumi, T. Ohno and M. Matsumura, *J. Photochem. Photobiol., A*, 2000, **132**, 99.
- A. Safrany, R. Gao and J. Rabini, *J. Phys. Chem. B*, 2000, **104**, 5848.
- M. Nirmal, B. O. Dabbousi, M. G. Bawendi, J. J. Macklin, J. K. Trautman, T. D. Harris and L. E. Brus, *Nature*, 1996, **383**, 802.
- T. Basche, *J. Lumen.*, 1998, **76/77**, 263.
- U. Bannin, M. Bruchez, A. P. Alivisatos, T. Ha, S. Weiss and D. S. Chemia, *J. Chem. Phys.*, 1999, **110**, 1195.
- R. G. Neuhauser, K. T. Shimizu, W. K. Woo, S. A. Empedocles and M. G. Bawendi, *Phys. Rev. Lett.*, 2000, **85**, 3301.
- M. Sugishaki, H.-W. Ren, K. Nishi and Y. Masumoto, *Phys. Rev. Lett.*, 2001, **86**, 4883.
- I. S. Osad'ko, *Chem. Phys.*, 2005, **316**, 99.
- B. R. Fisher, H.-J. Eisler, N. E. Stott and M. G. Bawendi, *J. Phys. Chem. B*, 2004, **108**, 143.
- X. Y. Wang, W. Q. Ma, J. Y. Zhang, G. J. Salamo, M. Xiao and C. K. Shih, *Nano Lett.*, 2005, **5**, 1873.
- A. Nakkiran, J. Thirumalai and R. Jagannathan, *Chem. Phys. Lett.*, 2007, **436**, 155.
- A. L. Efros and M. Rosen, *Phys. Rev. Lett.*, 1997, **78**, 1110.
- Burda, S. Link, M. Mohamed and M. El-Sayed, *J. Phys. Chem. B*, 2001, **105**, 12286.
- M. Shim, C. Wang and P. Guyot-Sionnest, *J. Phys. Chem. B*, 2001, **105**, 2369.
- M. Kuno, D. P. Fromm, S. T. Johnson, A. Gallagher and D. J. Nesbitt, *Phys. Rev. B*, 2003, **67**, 125304.
- K. T. Shimizu, R. G. Neuhauser, C. A. Leatherdale, S. A. Empedocles, W. K. Woo and M. G. Bawendi, *Phys. Rev. B*, 2001, **63**, 205316.
- J. Tang and R. A. Marcus, *J. Chem. Phys.*, 2005, **123**, 054704.
- G. Margolin and E. Barkai, *J. Chem. Phys.*, 2004, **121**, 1566.
- P. A. Frantsuzov and R. A. Marcus, *Phys. Rev. B*, 2005, **72**, 155321.
- M. Pelton, G. Smith, N. F. Scherer and R. A. Marcus, *Proc. Natl. Acad. Sci. U. S. A.*, 2007, **104**, 14249.
- J. J. Glennon, R. Tang, W. E. Buhro and R. A. Loomis, *Nano Lett.*, 2007, **7**, 3290.
- J. J. Glennon, W. E. Buhro and R. A. Loomis, *J. Phys. Chem. C*, 2008, **112**, 4813.
- H.-H. Kim, N. W. Song, T. S. Park and M. Yoon, *Chem. Phys. Lett.*, 2006, **432**, 200.
- T. Gensch, M. Bohmer and P. F. Armendia, *J. Phys. Chem. A*, 2005, **109**, 6653.
- Y. Xu and C. H. Langford, *J. Photochem. Photobiol., A*, 2000, **133**, 67.
- M. W. Holman, R. Liu and D. M. Adams, *J. Am. Chem. Soc.*, 2003, **125**, 12649.
- D. P. Colombo, Jr and R. M. Bowman, *J. Phys. Chem.*, 1995, **99**, 11752.
- N. Daude, C. Gout and C. Jouanin, *Phys. Rev. B*, 1977, **15**, 3229.
- P. M. Kumar, S. Badrinarayanan and M. Satry, *Thin Solid Films*, 2000, **358**, 122.
- R. F. Howe and M. Gratzel, *J. Phys. Chem.*, 1985, **89**, 4495.
- M. Gratzel, In “*Heterogeneous Photochemical Electron Transfer*”, CRC Press, Inc., Boca Raton, FL, USA, 1989, 117.
- M. Kuno, D. P. Fromm, H. F. Hamann, A. Gallagher and D. J. Nesbitt, *J. Chem. Phys.*, 2001, **115**, 1028.

Supplementary Information

Blinking Photoluminescence Properties of Single TiO₂ Nanodiscs : Interfacial Electron Transfer Dynamics

Ki-Seok Jeon, Seung-Do Oh, Yung Doug Suh, Hiroyuki Yoshikawa, Hiroshi Masuhara and Minjoong Yoon*, *Phys. Chem. Chem. Phys.* 2008, **xx**, xxxx

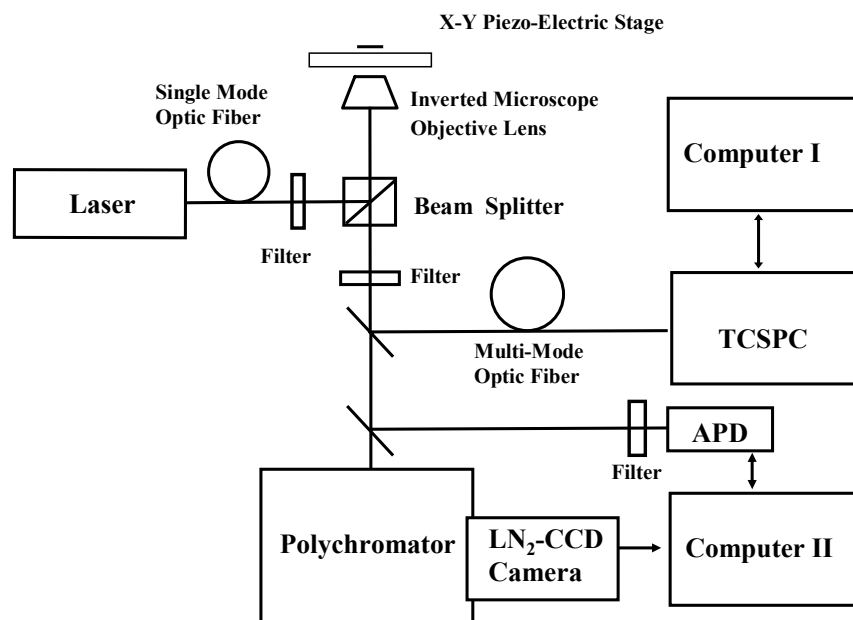
DOI: 10.1039/b00000x

Supplementary figure captions

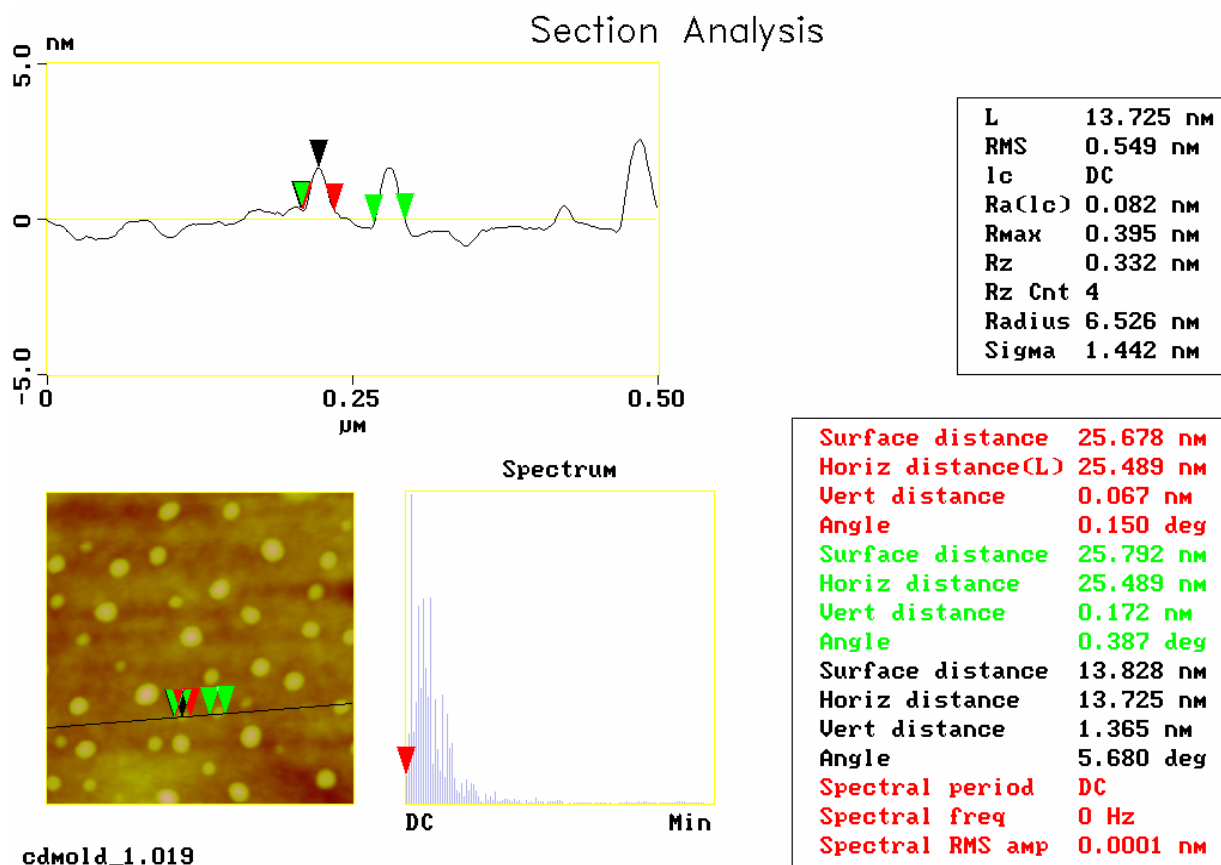
S-Fig. 1. Layout of laser scanning microscope-coupled fs-time-resolved PL system. The sample is mounted on a piezoelectric x,y scanning stage. Light from a laser is coupled into the single-mode optical fiber, illuminating the sample through the objective lens.

S-Fig. 2. AFM image and cross sectional analysis of TiO₂ nanodiscs.

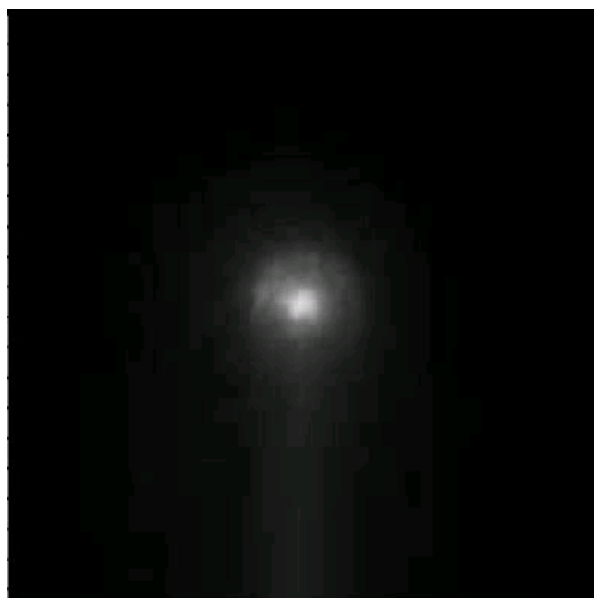
S-Fig. 3. Movie of PL blinking of TiO₂ nanodiscs (Separate video file is attached).



S-Fig. 1



S-Fig. 2



TiO₂ ND Video file.wmv

S-Fig. 3